

## Structure Analysis of Tropical Cyclone Phailin over Bay of Bengal using WRF Model

Ashik Imran\*<sup>1</sup>, Dr. Ishtiaque M. Syed<sup>1</sup>, Md. Shadikul Alam<sup>2</sup>, S.M. Quamrul Hassan<sup>2</sup>,  
M.A.K. Mallik<sup>2</sup>, Kh. Hafizur Rahman<sup>2</sup> and Md. Sanaul Hoque Mondal<sup>2</sup>

<sup>1</sup>Department of Physics, University of Dhaka

<sup>2</sup>Bangladesh Meteorological Department

\*Corresponding author: iamashikimran@gmail.com

**Abstract:** A Tropical cyclone (TC) is a warm core vortex in the troposphere. TCs can be characterized by deep convection and circulation of surface winds. Every year Bangladesh faces the most destructive TCs that form over Bay of Bengal (BoB). In this study, simulation of TC ‘Phailin (8<sup>th</sup>-14<sup>th</sup> October, 2013)’ that formed over BoB is conducted to investigate its horizontal and vertical structure and as well as the thermodynamics features of the TC by using WRF model. IMD and JTWC estimated data for the TC Phailin are used to certify the simulated outputs. Simulated maximum wind speed (MWS) at surface and minimum central pressure (MCP) are in good agreement with the estimated value. Horizontal size of the TC is very close to the average size of cyclones over NIO. Asymmetries are found in the structure of the TC from wind and relative vorticity distributions. In lower and mid troposphere the TC is associated with positive vorticity. Vertical wind distribution shows maximum wind of 70  $ms^{-1}$  between 850 and 750 hPa level. But the simulated system is intensified up to top troposphere (above 250 hPa) with wind speed around 40  $ms^{-1}$ . Very high RH (>60%) is found between 700 hPa and 500 hPa. Due to insufficient vertical observations over BoB, the vertical distributions of the simulated fields are compared with the theoretical values instead of any experimental justification.

**Key Words:** TC, vertical structure, IMD, JTWC, vorticity,

### 1. INTRODUCTION

The Bay of Bengal (BoB) is the largest bay in the world situated in northeastern part of the Indian Ocean that lies in the tropical belt. Cyclonic disturbance over this region is termed as ‘Tropical Cyclone (TC)’. These TCs have significant socio-economic impacts on the countries bordering the BoB. Therefore, it is very important to predict these cyclones with high accuracy to save valuable lives and wealth. The Indian subcontinent is one of the most horrible cyclone affected regions in the world. The subcontinent with a long coastline has experienced nearly 10 % of the global tropical cyclones. The mean annual temperature of the surface water of BoB is around 28°C [1] which is favorable for cyclone formation. Most of the TCs have their initial genesis over the BoB and strike Bangladesh coast (17%) and the east coast of India (58%) [2]. On an average, five to six TCs form every year, out of these two or three can be severe. The geographical structure of the BoB including shallow bathymetry, many river basins, poor socio-economic conditions and large population density along the coastal regions enhances the damage and loss of lives and properties due to TCs [3]. 90% of TC deaths are caused by storm surge which is the worst effect from a land falling cyclone [4]. In BoB, there are two cyclone seasons: the pre-monsoon; from April to June (28% of total cyclones occur in this season) and the post-monsoon from October to Dec. (almost 61 % occur in post-monsoon season) [5]. Tropical cyclones are characterized by a warm core vortex in the troposphere. It is the unique warm-core structure within a tropical cyclone that produces very strong winds near the surface and causes damage to coastal regions and islands through extreme wind driven storm surge, wave action and torrential rains [6].

In the mid-1950s, the development of a two dimensional axisymmetric hurricane model to understand the convective system is the beginning of numerical studies of TCs. The early numerical studies examined the role of latent heat release and the effect of convective parameterization in the structure of TCs. The intensity of a TC is controlled by the sea surface temperature, moisture distribution and vertical wind shear [7, 8]. The structure and intensity of TCs depend on heat from the rain bands [9, 10]. The size of a TC is determined by the initial vortex and initial latent heat flux. The size and hence the structure of the TCs are also influenced by the relative humidity distribution [11]. The TC ‘Nargis’ over BoB was simulated by Pattanaik and Rao in 2009 by using WRF model [12]. Pattanayak et al. (2008) made the comparative study of MM5 and WRF model in the simulation of TCs over Indian seas and showed that WRF model is better than MM5 [13]. Three new observation operators related to the TC track and structure- center position, velocity of storm motion, and surface axisymmetric wind structure—were used to construct a reasonable initial vortex in the high-resolution WRF model by Wu et al. in 2010 [14]. Deshpande et al. studied the ‘Odisha’ super cyclone (1999) and suggested that the intensity is sensitive to the Choice of CP schemes used in the model. They also found that KF (Kain-Fritsch) scheme gives better track and intensity prediction than other schemes [15]. In this present study WRF model is used to find the horizontal and

vertical structure and the associated thermodynamic features of VSCS ‘Phailin’ that formed over BoB from 8<sup>th</sup> to 14<sup>th</sup> October, 2013.

The Very Severe Cyclonic Storm (VSCS) ‘PHAILIN’ developed from a remnant cyclonic circulation over the South China Sea. The cyclonic circulation lay as a low pressure area over Tenasserim coast on 6<sup>th</sup> October, 2013. It moved west-northwestwards and intensified into a deep depression (DD) in the morning of 9<sup>th</sup> October and further into cyclonic storm (CS), ‘PHAILIN’ with maximum sustained wind speed of 35 Knots ( $18 \text{ ms}^{-1}$ ) in the evening of the same day near  $13.6^{\circ}\text{N}$  and  $92.5^{\circ}\text{E}$ . Moving northwestwards, the system intensified into a severe cyclonic storm (SCS) at 0830 UTC of 10<sup>th</sup> October with maximum sustained wind speed of 55 Knots ( $28.29 \text{ ms}^{-1}$ ). It intensified into a VSCS at 1130 UTC of the same day over east central BoB. The system continued to intensify further and attained its maximum intensity of 115 knots ( $59.16 \text{ ms}^{-1}$ ) in the morning of 11<sup>th</sup> October. The system crossed Andhra Pradesh & Odisha coast around 2230 UTC of 12<sup>th</sup> October, 2013. After landfall, the system weakened gradually into an SCS at 0830 UTC, into a CS at 1130 UTC and into a DD over north Chhattisgarh at 1730 UTC of 13<sup>th</sup> October. It became a D at 0300 UTC and a well-marked low pressure area over southwest Bihar and neighborhood [16] at 1430 UTC of 14<sup>th</sup> October. The observed track of the system is shown in Fig. 1.

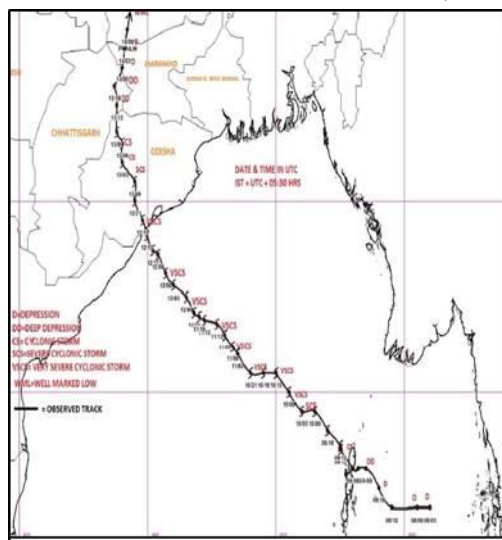


Fig. 1: Observed track of VSCS PHAILIN [16]

## 2. EXPERIMENTAL SET UP & METHODOLOGY

### 2.1 Data used

The  $1.0^{\circ} \times 1.0^{\circ}$  resolution Global Final (FNL) Analysis data provided by the National Centre for Environmental Prediction (NCEP) has been taken as the initial and lateral boundary condition. The model simulated minimum central pressure, maximum wind speed at surface are compared with the estimated value from India Meteorological Department (IMD) and joint Typhoon Warning Center Data.

### 2.2 Model Experimental Setup

In this study, the simulation of cyclone Phailin (08<sup>th</sup>-14<sup>th</sup> October, 2013) over the BoB is done to analyze its structure. The mesoscale model used in this study is the WRF-ARW model. The model consists of fully compressible non-hydrostatic equations and different prognostic variables are utilized. The model vertical coordinate is terrain following hydrostatic pressure. The horizontal grid is Arakawa C-grid staggering. The experiment has been done on single domain with 20 km horizontal grid resolution. The domain configuration is given in Fig. 2. The details of the model and domain configuration are listed in Table 1.

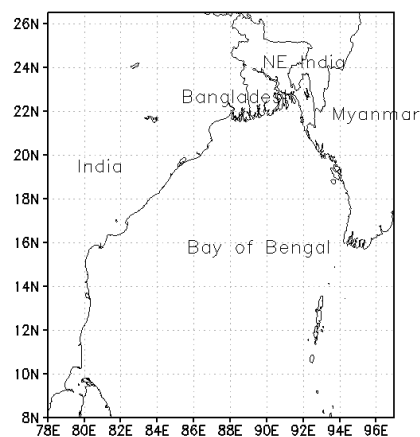


Fig. 2: WRF Model Domain for the NWP

Table 1: WRF Model and Domain Configurations

<b>No. of domain</b>	1	<b>Horizontal grid</b>	Arakawa C-grid
<b>Center of the domain</b>	$17.5^{\circ}\text{N}, 87.5^{\circ}\text{E}$	<b>Time integration</b>	3 <sup>rd</sup> order Runge-Kutta
<b>Resolution</b>	20 km	<b>Initial conditions</b>	3-D real-data (FNL: $1^{\circ} \times 1^{\circ}$ )
<b>Vertical co-ordinate</b>	40 sigma levels	<b>Microphysics</b>	WSM 6-class (Hong and Lim)
<b>No. of grid points</b>	W-E 100, S-N 100	<b>CP scheme</b>	Kain-Fritsch (new Eta)
<b>Run time (72 hrs)</b>	2013-10-10_00 to 2013-10-13_00	<b>PBL scheme</b>	Yonsei University Scheme (YSU)
<b>Map projection</b>	Mercator	<b>Radiation scheme</b>	RRTM long wave; Dudhia's short wave

### 3. RESULT AND DISCUSSION

Structure of tropical cyclone Phailin is analyzed by using WRF model and simulated parameters are visualized by using Grid analysis and Display System (GrADS). The simulated results and the associated discussions are represented in the following sub-sections.

#### 3.1 ANALYSIS OF MEAN SEA LEVEL PRESSURE

A comparison between the time evolution of the estimated central pressure (ECP) [16] and simulated minimum central pressure (MCP) of the TC Phailin is shown in Fig. 3. The ECP and simulated MCP gradually drop with time up to peak intensity and then the two pressures increase with time. The ECP falls more sharply than the simulated MCP. The lowest simulated MCP is 949 hPa at 0000 UTC of 12<sup>th</sup> October and the lowest ECP is 940 hPa from 0300 UTC of 11<sup>th</sup> October to 1500 UTC of 12<sup>th</sup> October. Therefore, model has predicted the intensification of the system 21 hours in delay and underestimates in pressure falling by 9 hPa. On 12<sup>th</sup> October, 1500 UTC to 2100 UTC estimation depicts very sharp rise in pressure and the value is 26 hPa in 06 hours. But the model is unable to capture this phenomenon.

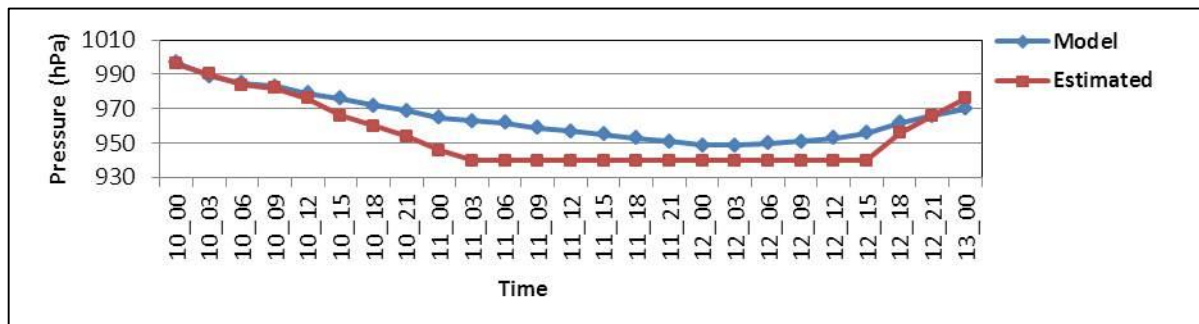


**Fig. 3:** Comparison of model simulated MCP (hPa) of the TC Phailin with the estimated central pressure (hPa)

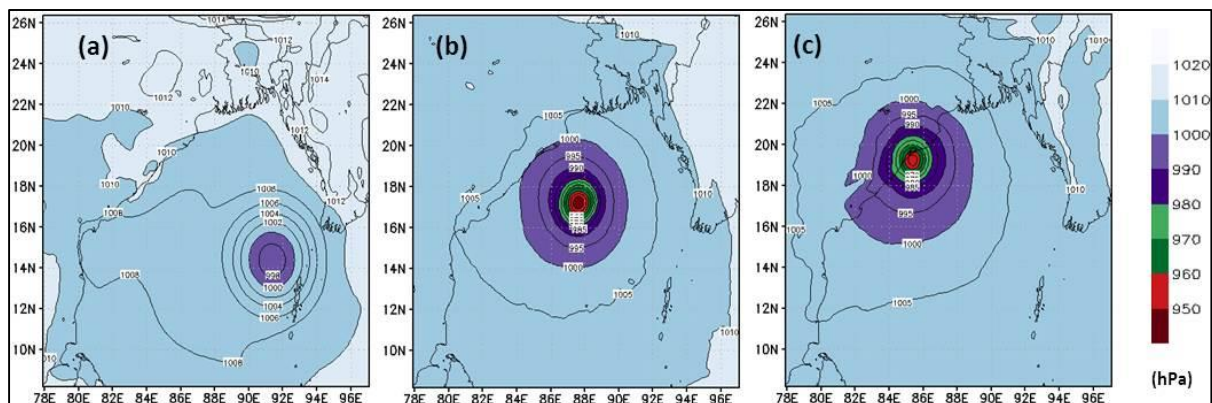


**Fig. 4:** Distribution of MSLP (hPa) based on 0000 UTC of 10<sup>th</sup> October, 2013 and valid for (a) 0000 UTC of 10<sup>th</sup> October, (b) 2100 UTC of 11<sup>th</sup> October (maximum intensity), and (c) 1500 UTC of 12<sup>th</sup> October, 2013.

The distributions of simulated MSLP for the TC Phailin at 0000 UTC of 10<sup>th</sup>, 2100 UTC of 11<sup>th</sup> (maximum intensity), and 1500 UTC of 12<sup>th</sup> October, 2013 are shown in Fig. 4 (a-c). The figure shows that the intensity of the TC increases as the MSLP decreases with time up to its maximum intensity and the system changes its position with time. Different locations of the system at different times indicate the northwestward movement of the system. The isobaric lines are in circular arrangement around the center (eye) of the TC and there are some asymmetry properties in the outer periphery. At the stage of maximum intensity (Fig. 4b), considering the outermost closed isobar, the system's horizontal size is estimated around 6.3° (680 km) in the E-W direction and 6.1° (670 km) in the N-S direction. The difference in horizontal sizes demonstrates the spatial asymmetry in its horizontal structure.

#### 3.2 ANALYSIS OF WIND FLOW

##### 3.2.1 WIND AT SURFACE LEVEL

Fig. 5 shows the temporal variations of simulated maximum wind speed (MWS) and estimated [16] maximum sustained surface wind of the TC Phailin. The simulated MWSs are evaluated at the standard meteorological height of 10 m. The model underestimates the MWS most of the times in the evolution. The simulated highest MWS of 43 ms<sup>-1</sup> is obtained at 2100 UTC of 11<sup>th</sup> October and the estimated maximum sustained surface wind is 59.16 ms<sup>-1</sup> at 0300 UTC of 11<sup>th</sup> October and maintained this speed for next 36 hours. So, the model

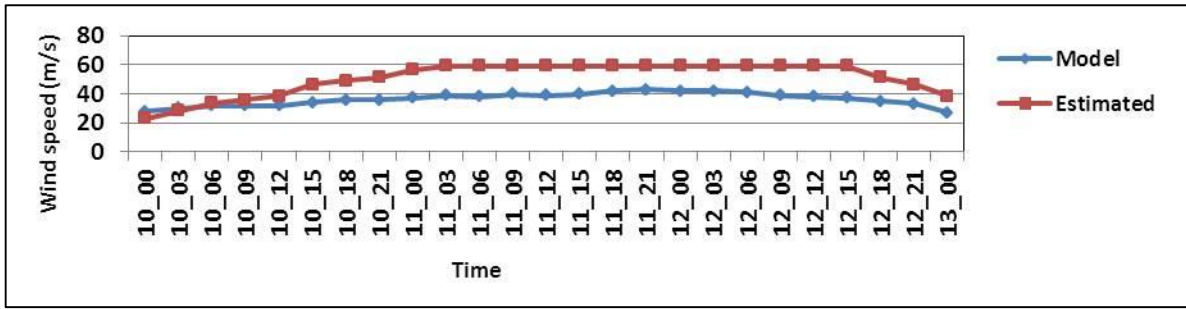


**Fig. 5:** Comparison of simulated MWS ( $\text{ms}^{-1}$ ) at surface with the estimated maximum sustained surface wind ( $\text{ms}^{-1}$ ) [16].

underestimates the highest MWS by nearly  $16\text{ms}^{-1}$ . After that, both the winds gradually decrease with time. The model prediction in highest MWS is 18 hours in delay than estimation. After peak intensity, the estimated wind speed falls more sharply than the simulation.

### 3.2.2 WIND AT 850 hPa & 200 hPa LEVEL

The horizontal distributions of wind associated with the TC Phailin at 850 hPa and 200 hPa level at 0000 UTC of 10<sup>th</sup>, 2100 UTC of 11<sup>th</sup> (maximum intensity), and 1500 UTC of 12<sup>th</sup> October, 2013 are represented in Fig. 6 and Fig. 7 respectively. At 850 hPa level, strong cyclonic circulation is found in every stage of wind distribution that is evident for the inflow in lower level. The wind field is asymmetric in the horizontal distribution at 0000 UTC of 10<sup>th</sup> October, 2013. The distribution depicts a well-organized eye and the stronger wind is found in the south-southwest sector of the system. At the stage of maximum intensity (Fig. 6b), the TC is more organized with almost uniform wind band around a well-organized eye and the wind speed has a value exceeding  $60\text{ms}^{-1}$ . At the time of landfall the wind distribution is nearly uniform with a little asymmetry in the front side of the system. At 200 hPa (Fig. 7), there is a center of anticyclonic circulation roughly at  $18^{\circ}\text{N}$  and  $80^{\circ}\text{E}$ . There is another anticyclonic circulation with center at  $14^{\circ}\text{N}$  and  $94^{\circ}\text{E}$ . The system becomes more intense (well-organized) with increasing

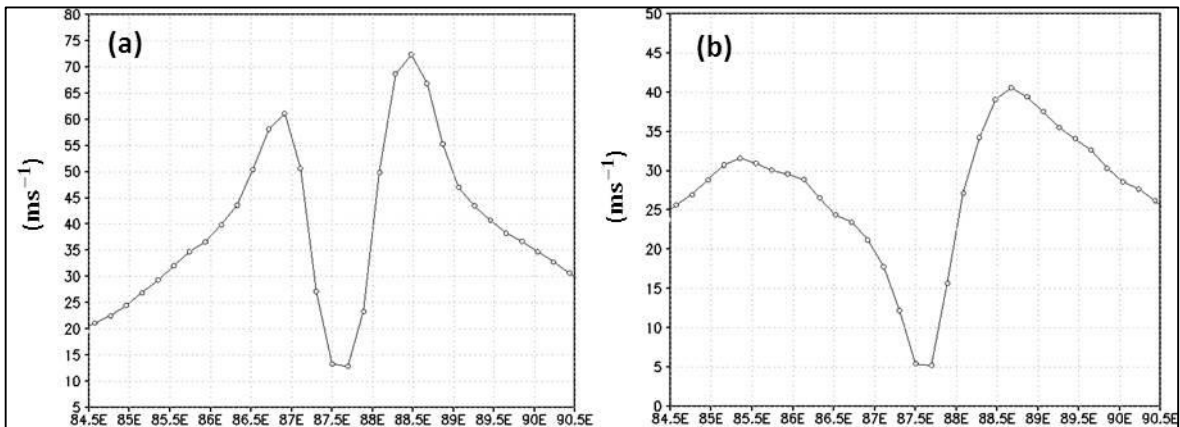


**Fig. 6:** Wind distribution (speed in  $\text{ms}^{-1}$ ) at 850 hPa l based on 0000 UTC of 10<sup>th</sup> Oct. and valid for (a) 0000 UTC of 10<sup>th</sup> Oct., (b) 2100 UTC of 11<sup>th</sup> Oct. (maximum intensity), and (c) 1500 UTC of 12<sup>th</sup> Oct., 2013.

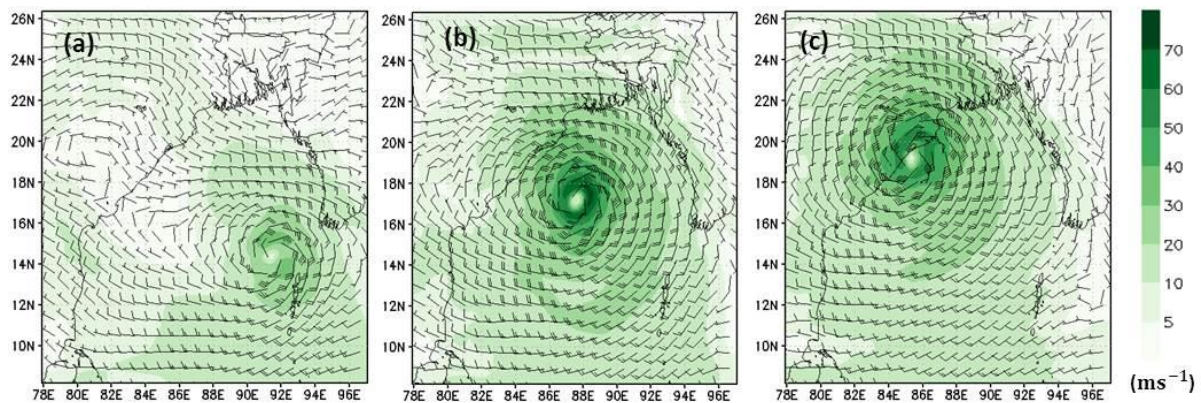


**Fig. 7:** Wind distribution (speed in  $\text{ms}^{-1}$ ) at 200 hPa based on 0000 UTC of 10<sup>th</sup> Oct. and valid for (a) 0000 UTC of 10<sup>th</sup> Oct., (b) 2100 UTC of 11<sup>th</sup> Oct. (maximum intensity), and (c) 1500 UTC of 12<sup>th</sup> Oct., 2013.

time. At the mature stage (2100 UTC 11<sup>th</sup> October), the system intensified into a VSCS and the cyclonic circulation associated with the system is extended vertically up to 200 hPa level. There is a strong cyclonic circulation around the center with an anticyclonic circulation to the east of the system. This anticyclonic circulation over north northwestern side of the system maintains the southeasterly movement of the system. A trough to the west of the system helps the system to move north-westward. At the time of landfall (1500 UTC of 12<sup>th</sup> October), the system is found less intense.

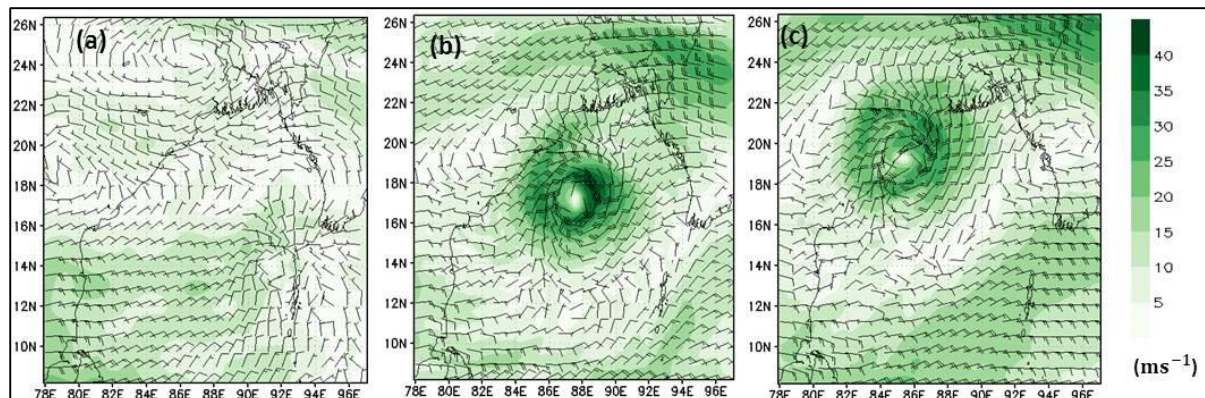
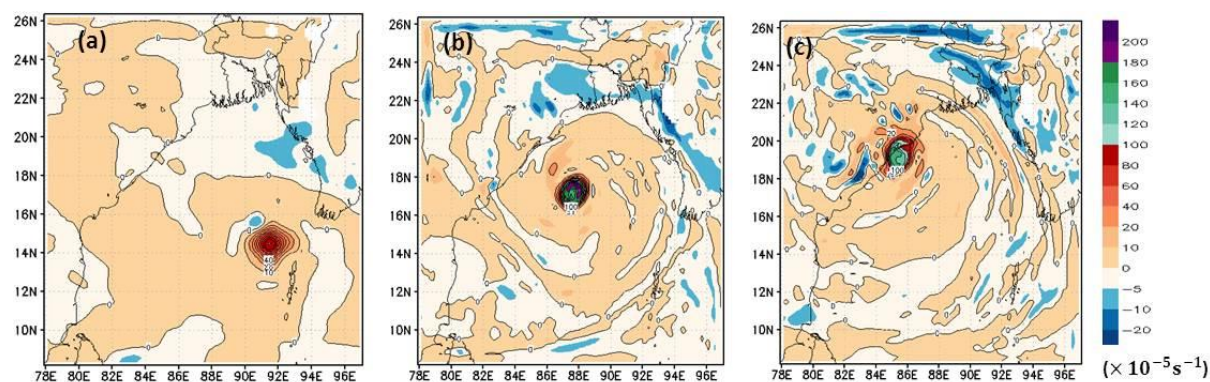


**Fig. 8:** E-W sectional view of wind speed ( $\text{ms}^{-1}$ ) at (a) 850 hPa and (b) 200 hPa based on 0000 UTC of 10<sup>th</sup> October and valid for 2100 UTC of 11<sup>th</sup> October (maximum intensity), 2013, when the system center is at  $17.31^{\circ}\text{N}$  and  $87.70^{\circ}\text{E}$ .

Figures 8a and 8b show the distributions of the simulated wind at 850 hPa and 200 hPa level along E-W sectional view passing through its center ( $17.31^{\circ}\text{N}$  and  $87.70^{\circ}\text{E}$ ) at 2100 UTC of 11<sup>th</sup> October, 2013 (maximum intensity). From the figure, the central region is relatively calm and this region is surrounded with maximum wind. According to the model, at 850 hPa, the radius of maximum wind ( $72 \text{ms}^{-1}$ ) of the system is found to be around 96 km. There is a little asymmetry in the wind distribution at 850 hPa level. At 200 hPa, the system is extended in size with roughly 116 km radius of maximum wind ( $40 \text{ms}^{-1}$ ) and the asymmetry in the wind distribution is relatively larger.

### 3.3 ANALYSIS OF RELATIVE VORTICITY

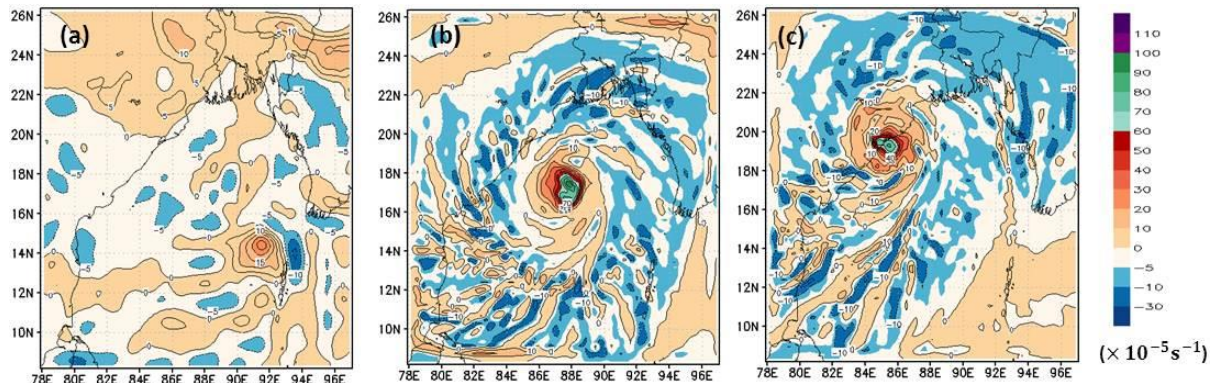
The Fig. 9-10 represent the horizontal distributions of model simulated relative vorticity for 850 hPa and 200 hPa levels respectively at 0000 UTC of 10<sup>th</sup>, 2100 UTC of 11<sup>th</sup> (maximum intensity), and 1500 UTC of 12<sup>th</sup> October, 2013. It is seen from the figures that the center of the system is associated with maximum relative vorticity and it is positive for all the levels. The values of relative vorticity decrease as the distance from center increases. Also the values of positive relative vorticity show an increasing trend with time i.e. the system is associated with increasing vorticity following the development of the TC. From the distributions, it is found that larger vorticity is found in the western part of the system that helps the system to move in a westward direction. At the time of landfall the relative vorticity starts decreasing. At 850 hPa, at the stage of maximum intensity the relative vorticity at the system center is  $200 \times 10^{-5} \text{s}^{-1}$ . The distribution is in circular pattern. There are very small negative vorticities far away from the center. The positive values of relative vorticity in the northern hemisphere correspond to cyclonic circulation and negative values of vorticity correspond to anticyclonic circulation. The positive values of relative vorticity at lower levels are clearly the indication of strong cyclonic circulation at these levels. This



**Fig. 9:** Distribution of relative vorticity (unit:  $\times 10^{-5} \text{s}^{-1}$ ) at 850 hPa based on 0000 UTC of 10<sup>th</sup> October, and valid for (a) 0000 UTC of 10<sup>th</sup> October, (b) 2100 UTC of 11<sup>th</sup> Oct. (maximum intensity), and (c) 1500 UTC of 12<sup>th</sup> October, 2013.

cyclonic circulation contributes to the severe convective activities i.e. there is a supply of moisture into the system which is essential for the system to maintain its intensity.

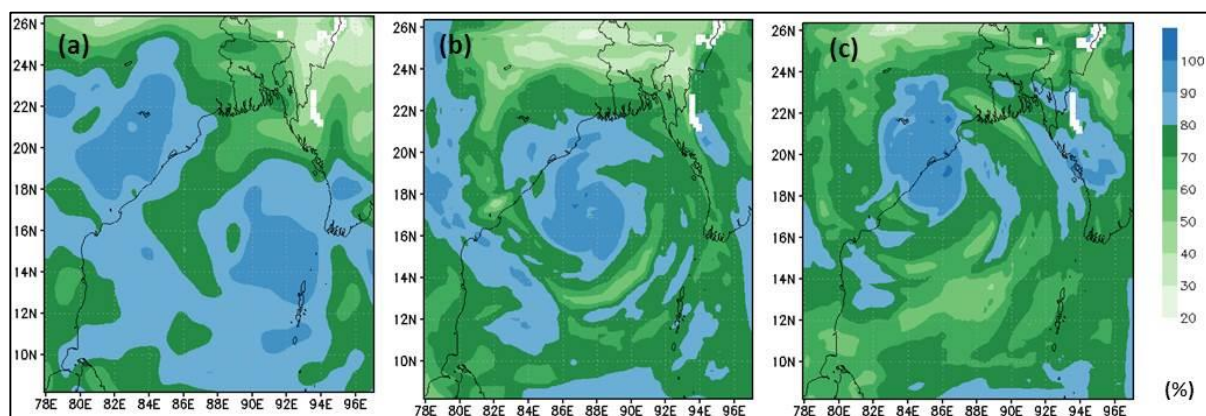
At 200 hPa level, the values of positive relative vorticity are smaller than that of at lower levels and the values of negative vorticity increase (above  $30 \times 10^{-5} \text{s}^{-1}$ ). The maximum positive vorticity is roughly  $110 \times 10^{-5} \text{s}^{-1}$  around the center. The distance of negative vorticity distribution from the system center is decreased. The weak positive vorticity is jointly distributed with negative vorticity at 200 hPa level. The negative values of vorticity at this level indicate strong anticyclonic circulation and hence the outflow of winds.



**Fig. 10:** Distribution of relative vorticity (unit:  $\times 10^{-5} \text{s}^{-1}$ ) at 200 hPa based on 0000 UTC of 10<sup>th</sup> October, and valid for (a) 0000 UTC of 10<sup>th</sup> October, (b) 2100 UTC of 11<sup>th</sup> October (maximum intensity), and (c) 1500 UTC of 12<sup>th</sup> October, 2013.

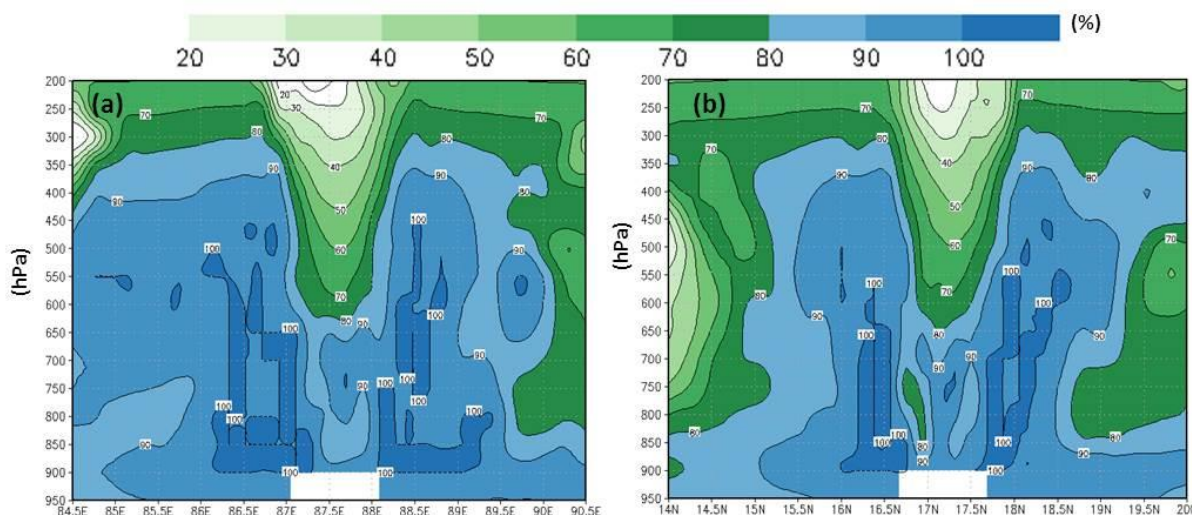
### 3.4 HORIZONTAL & VERTICAL DISTRIBUTIONS OF RELATIVE HUMIDITY (RH)

Fig. 11 presents the horizontal distributions of RH for the TC Phailin at 850 hPa level based on 0000 UTC of 10<sup>th</sup> October and valid for 0000 UTC of 10<sup>th</sup>, 2100 UTC of 11<sup>th</sup> (maximum intensity), and 1500 UTC of 12<sup>th</sup> October, 2013. The distributions show that the TC is associated with high RH of the order of 80 % or more. This high RH distribution moves continuously northwestward (southeasterly flow) along with the system. Huge amount of moisture with a value of around 80-100 % is supplied along with the existing strong southeasterly flow over southeastern coast of India (Odisha and Andhra Pradesh). Severe convective activities affiliated with the cyclonic system occur due to this high RH that gives heavy rainfall in the coastal regions at the time of landfall. The vertical distribution of RH at the stage of maximum intensity (2100 UTC of 11<sup>th</sup> October) (a) along 17.31°N (E-W sectional view) and (b) along 87.70°E (N-S sectional view) are shown in Fig. 12. The central region of the system is associated with lower values of RH than the surroundings from mid to upper troposphere. Along the central region, high RH (80 % or more) is extended vertically up to 600 hPa. Above 600 hPa the values of RH is decreasing and the air becomes more dry (RH less than 50 %) above 400 hPa. But RH of the order of 80 to 100 % in the peripheral region i.e. along the rain bands is extended vertically upward up to 350 hPa and relative humidity of around 70 % is maintained above 350 hPa level of the troposphere. In the horizontal directions, the distribution of large RH is extended along the movement of the system (towards the north-west direction) because air pressure is reduced due to large amount of vapor (high RH) and a cyclonic system moves towards the low



**Fig. 11 :** The distribution of relative humidity (%) at 850 hPa level based on 0000 UTC of 10<sup>th</sup> October and valid for (a) 0000 UTC of 10<sup>th</sup> October, (b) 2100 UTC of 11<sup>th</sup> October (maximum intensity), and (c) 1500 UTC of 12<sup>th</sup> October, 2013.

pressure area. There is inflow of dry air from the west at top tropospheric levels and also from south at mid tropospheric levels.



**Fig. 12:** Relative humidity (%): (a) east-west sectional view and (b) north-south sectional view at 2100 UTC of 11<sup>th</sup> October (maximum intensity), 2013, when the system center is at 17.31°N and 87.70°E.

### 3.5 ANALYSIS OF ZONAL & MERIDIONAL COMPONENTS OF VELOCITY

Fig. 13 indicate the vertical distributions of (a) zonal and (b) meridional wind at the maximum intensity stage (2100 UTC of 11<sup>th</sup> October) when the system center is at 17.31°N and 87.70°E. A relatively calm wind with magnitude less than  $5 \text{ ms}^{-1}$  is detected along the center of the system which is the eye of the TC. The development of this calm region is from the lower to upper troposphere. The eye is encircled by strong winds along the eyewall. These winds are decreasing with increasing height i.e. strong winds with different magnitudes are confined to

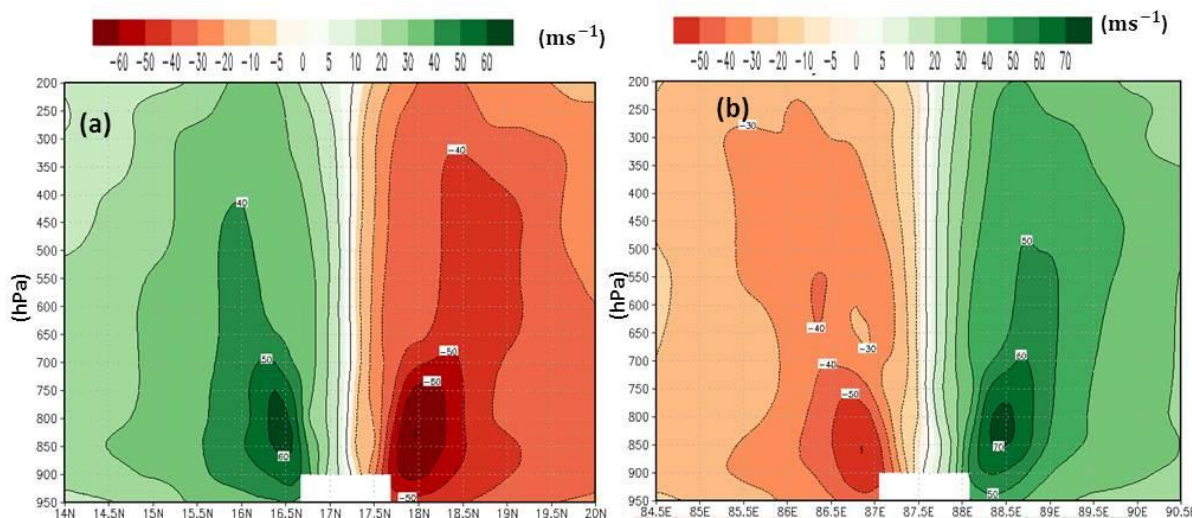


**Fig. 13:** (a) Zonal and (b) Meridional component of velocity ( $\text{ms}^{-1}$ ) at 2100 UTC of 11<sup>th</sup> October (maximum intensity), 2013, when the system center is at 17.31°N and 87.70°E.

different tropospheric levels. The magnitudes of winds are also decreasing with increasing distance from the center in the horizontal directions. From Figure 13a, winds flow in an easterly direction (negative) in the northern side of the system and in a westerly direction (positive) in the southern side. These strong easterly and westerly winds indicate deep inflow in the lower and mid tropospheric levels. Maximum wind of  $60 \text{ ms}^{-1}$  is observed on both sides of the center that extends vertically up to approximately 750 hPa level. But the horizontal extension of this maximum wind is larger in the northern side of the system. So, there is an asymmetry between the south and north sector of the system. Winds with magnitudes about  $30 \text{ ms}^{-1}$  are extended above 200 hPa level on both sides. From meridional wind distribution (Figure 13b), there are southerly winds (positive) in the east and northerly winds (negative) in the west of the system indicating inflow of winds. There is one maximum of winds of  $70 \text{ ms}^{-1}$  from 850 hPa to 750 hPa to the east and another maximum of  $50 \text{ ms}^{-1}$  from 950 hPa to 750 hPa to the west of the center. At around 200 hPa level, strong winds of  $40 \text{ ms}^{-1}$  are found to the east and winds of  $30 \text{ ms}^{-1}$  are

found to the west of the center. So, there is a clear indication of asymmetry between the east and west part of the system.

### 3.6 ANALYSIS OF VERTICAL COMPONENT OF VELOCITY

Fig. 14 indicates the distributions of vertical velocity component at the stage of maximum intensity (at 2100 UTC of 11<sup>th</sup> October) along 17.31°N (E-W sectional view (a)) and along 87.70°E (N-S sectional view (b)). From the E-W sectional view it is evident that vertical velocities range roughly from  $-0.2$  to  $2.0$   $\text{ms}^{-1}$  and it is roughly from  $-0.3$  to  $2.7$   $\text{ms}^{-1}$  in the N-S sectional view. In the E-W view, we found a strong upward motion of around  $2$   $\text{ms}^{-1}$  to the east of the center. This strong updraft is along the peripheral region and extends from mid to upper troposphere. In the west, maximum upward speed of about  $1.2$   $\text{ms}^{-1}$  is evident in between lower and mid troposphere. In the N-S view, maximum updraft of around  $2.7$   $\text{ms}^{-1}$  is found to the south of the center from 500 to 300 hPa. These upward motions with different magnitudes at different parts of the system through the troposphere feed necessary moisture to the system and hence help the system to be more intense. Comparatively stronger upward motion is evident in the south-east sector of the system. In both figures, there is an indication of sinking air through the center of the TC. The regions in between rain bands also show some downdrafts.

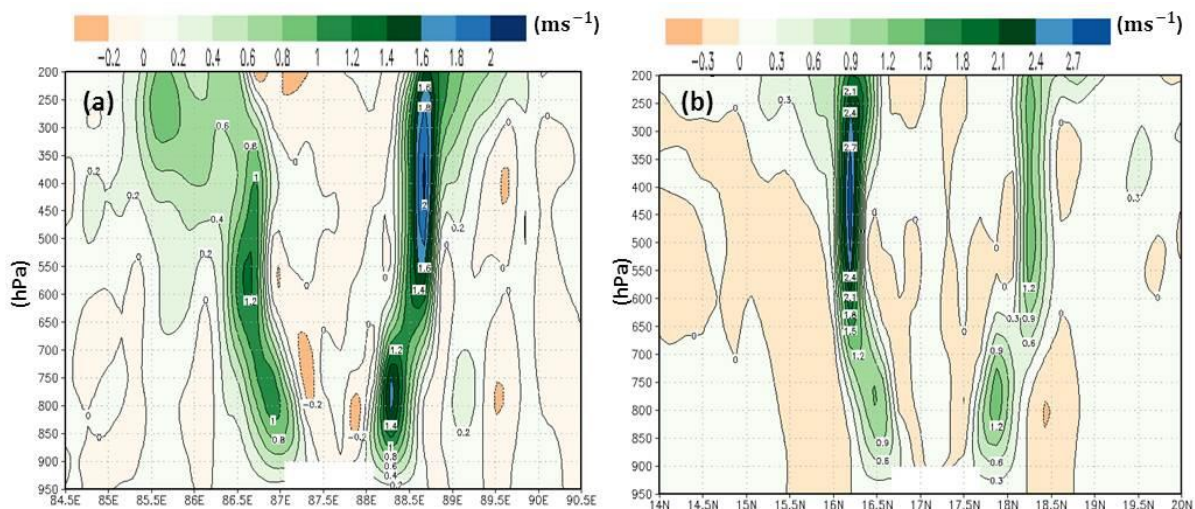


**Fig. 14:** Vertical component of velocity ( $\text{ms}^{-1}$ ): (a) east-west sectional view and (b) north-south sectional view at 2100 UTC of 11<sup>th</sup> October (maximum intensity), 2013, when the system center is at 17.31°N and 87.70°E.

### 3.7 LATENT HEAT FLUX ANALYSIS

Fig. 15 represents the distributions of latent heat flux at surface associated with the TC Phailin. In the formative stage (Fig. 15a), uniform distribution of latent heat flux ( $600\text{--}700$   $\text{Wm}^{-2}$ ) is found around the center. The minimum latent heat flux is found at the calm central region. The distance of the uniform latent heat distribution is roughly 50 km from the center, where the wind speed is at maximum with a uniform distribution (Fig. not shown). Therefore, the strongest wind and maximum latent heat flux maintain relatively the same position. The supply of latent heat continues as long as the system is over the bay, and the latent heat flux is increased to reach

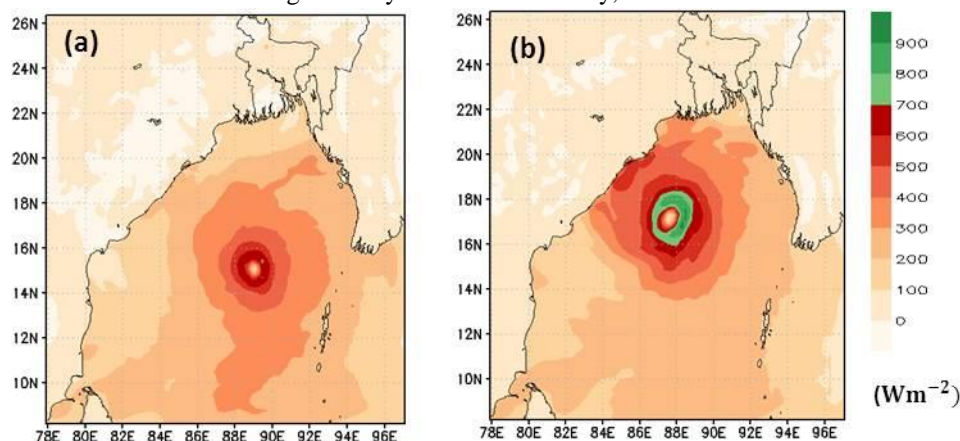


**Fig. 15:** The distribution of latent heat flux ( $\text{Wm}^{-2}$ ) at surface, based on 0000 UTC of 10<sup>th</sup> October, 2013 and valid for (a) 0000 UTC of 11<sup>th</sup> October (Formative stage) and (b) 2100 UTC of 11<sup>th</sup> October (Maximum intensity stage), 2013.

its maximum value at the stage of maximum intensity. At the stage of maximum intensity (Fig. 15b), there is a band of latent heat flux around the center (70 km from the center) and maximum latent heat flux ( $800\text{-}900\text{ Wm}^{-2}$ ) is found in the east part of the system that makes the wind in this part of the system strongest. The maximum supply of latent heat along the eastern part of the system makes the wind in this region strongest which is supported by the strong upward motion along the east sector of the TC, (vertical velocity component in Fig. 14a). The positive latent heat flux indicates the gain of energy from the warm ocean surface to the atmosphere.

#### 4. CONCLUSION

1. The simulated and estimated lowest central pressure for the TC Phailin are 949 hPa and 940 hPa (IMD and JTWC data) respectively. Therefore, the model underestimates in pressure falling by only 9 hPa. Moreover, the model has predicted the intensification of the system 21 hours in delay.
2. Average horizontal size (675 km) of the cyclone at the stage of maximum intensity is very close found to the average size of cyclones (300-600 km) over the north Indian seas.
3. At surface, the highest simulated maximum wind is  $43\text{ ms}^{-1}$ . IMD and JTWC estimated maximum sustained surface wind of the TC Phailin is  $59\text{ ms}^{-1}$ . Therefore, the model underestimates in maximum wind speed by  $16\text{ ms}^{-1}$ .
4. At 850 hPa and 200 hPa, radius of maximum wind (at the stage of maximum intensity) are respectively around 96 km (wind speed  $72\text{ ms}^{-1}$ ) and 116 km (wind speed  $40\text{ ms}^{-1}$ ). So, the wind speeds associated with a TC decrease with increasing height but the size increases.
5. Inflows (cyclonic circulation) and outflows (anti-cyclonic circulation) of wind in lower and upper troposphere respectively are found from the distributions of wind and relative vorticity at 850 hPa and 200 hPa. These distributions also capture the asymmetries in the horizontal structure of the TC.
6. Relative humidity with magnitudes 60-100 % is found between 700 and 500 hPa level (at the stage of maximum intensity) that favors the intensification of the cyclonic system Phailin.
7. Model depicts large vertical extension (up to the upper troposphere) of the TC Phailin. The system is most strong between 850-750 hPa where the winds are around  $70\text{ ms}^{-1}$ . Relatively strong winds with magnitude  $40\text{ ms}^{-1}$  are found around 200 hPa.
8. Moisture supply to the system is maintained through strong upward motion of the order of  $0.2\text{-}2.7\text{ ms}^{-1}$ .
9. The strongest wind associated with the TC Phailin is found where the latent heat flux is maximum.

#### Acknowledgements

The authors are grateful to NCAR for providing the WRF model. We are also indebted to NCEP, IMD and JTWC for providing the analysis data sets and required observed data. We are also thankful to Department of Physics, Dhaka University and Bangladesh Meteorological Department for the technical support. We thankfully acknowledge Ministry of Science and Technology-Government of the People's Republic of Bangladesh for providing the financial assistance to fulfill this study.

#### References

- [1] BANGLAPEDIA, 2006; <https://en.wikipedia.org/wiki/Banglapedia>
- [2] RSMC, NEW DELHI; [www.imd.gov.in](http://www.imd.gov.in)
- [3] U. C. MOHANTY, KRISHNA K. OSURI and SUJATA PATTANAYAK, 2013: A study on high resolution mesoscale modeling systems for simulation of tropical cyclones over the Bay of Bengal. *MAUSAM*, 64, 1, 117-134.
- [4] James M. Shultz, Jill Russell and Zelde espinel, 2005: Epidemiology of Tropical Cyclones: The Dynamics of Disaster, Disease, And Development. *Oxford Journal*, doi: <https://doi.org/10.1093/epirev/mxi011>.
- [5] Singh, O., Ali Khan, T. & Rahman M., 2000: Changes in the frequency of tropical cyclones over the North Indian Ocean; *Meteor. Atmos. Phys.*, 75: 11. doi: 10.1007/s007030070011.
- [6] Henderson-Sellers, A., H. Zhang, G. Berz, K. Emanuel, W. Gray, C. Landsea, G.Holland, J. Lighthill, S. L. Shieh, P. Webster and K. McGuffie, 1998: Tropicalcyclones and global climate change: A post-IPCC assessment, *Bulletin of the Amer. Meteor. Soc.*, 79, 19-38.
- [7] Wang, Y., and C.-C. Wu, 2004: Current understanding of tropical cyclone structure and intensity changes -A review, *Meteor. Atmos. Phys.*, 87, 257-278.
- [8] Gray, W. M., 1968: Global view of the origin of tropical disturbances and storms. *Mon. Wea. Rev.*, 96, 669-700.
- [9] Wu, C.-C., H.-J. Cheng, Y. Wang, and K.H. Chou, 2009: A numerical investigation of the eyewall evolution of a land falling typhoon, *Mon. Wea. Rev.*, 137, 21-40.

- [10] Moon, Y., and D. S. Nolan, 2010: The dynamic response of the hurricane wind field to spiral rainband heating, *J. Atmos. Sci.*, 67, 1779–1805.
- [11] Hill, K.A., and G.M., Lackmann, 2009: Influence of environmental humidity on tropical cyclone size, *Mon. Wea. Rev.*, 137, 3294–3315.
- [12] Pattanaik, D. R. and Rama Rao, Y. V. 2009: Track prediction of very severe cyclone ‘Nargis’ using high resolution weather research forecasting (WRF) model, *J. Earth Syst. Sci.* 118, No. 4, August 2009, 309–329.
- [13] Pattanaik, S., and U.C. Mohanty, 2008: A comparative study on performance of MM5 and WRF models in simulation of tropical cyclones over Indian seas, *Current Sci.*, 95(7), 923–936.
- [14] Chun-Chieh Wu and Guo-Yuan Lien 2010: Assimilation of Tropical Cyclone Track and Structure Based on the Ensemble Kalman Filter (EnKF). *J. Atmos. Sci.*, 67, 3806-3822; doi: 10.1175/2010jas3444.1.
- [15] Deshpande, M. S., S. Pattnaik, and P. S. Salvekar, 2012: Impact of cloud parameterization on the numerical simulation of a super cyclone, *Ann. Geophys.*, 30, 775-795, doi: 10.5194/angeo-30-775-2012
- [16] Very Severe Cyclonic Storm, PHAILIN over the Bay of Bengal (08-14 October 2013): A Report; Cyclone Warning Division India Meteorological Department New Delhi October 2013. [www.imd.gov.in](http://www.imd.gov.in)